J Prev Alz Dis 2023;3(10):581-594
Published online May 3, 2023, http://dx.doi.org/10.14283/jpad.2023.56

Original Research

Neuroprotective Effects of IVIG against Alzheimer' s Disease via Regulation of Antigen Processing and Presentation by MHC Class I Molecules in 3xTg-AD Mice

Z. Fei, B. Pan, R. Pei, S. Ye, Z. Wang, L. Ma, R. Zhang, C. Li, X. Du, H. Cao

Institute of Blood Transfusion, Chinese Academy of Medical Sciences and Peking Union Medical College, Chengdu, China

Corresponding Author: Xi Du and Haijun Cao , Institute of Blood Transfusion, Chinese Academy of Medical Sciences and Peking Union Medical College, Chengdu 610052, China, shela44@163.com; chjr007@163.com. Tel: 86-28-61648527

Abstract

BACKGROUND: The results of clinical trials for Alzheimer's disease (AD) patients treated with Intravenous immunoglobulin (IVIG) revealed inconsistency in efficacy.

OBJECTIVE: To explore the neuroprotective effects and possible mechanisms of different IVIG in 3xTg-AD mice.

METHODS: 3-month-old 3xTg-AD mice were administered intraperitoneally with different IVIG (A/B/C) for 3 months and then the therapeutic effects were observed and tested at 9 months of age. The bioavailability of IVIG and Aβ40/42 concentrations in parietotemporal cortex was measured by ELISA. Behavioral tests were performed to examine cognitive functions. Immunohistochemistry was utilized to examine the deposition of Aβ, the phosphorylation of tau, the levels of GFAP and Iba-1 in the hippocampus. Proteomics, Luminex assay and parallel reaction monitoring were performed to identify and verify the proteins that showed a marked change in the hippocampus.

RESULTS: IVIG-C was more effective than IVIG-A and IVIG-B in counteracting cognitive deficits, ameliorating Aβ deposits and tau phosphorylation, attenuating the activation of microglia and astrocytes in the hippocampus and inhibiting the secretion of pro-inflammatory factors. IVIG-C affected innate immunity and suppressed the activation of antigen processing and presentation by MHC class I molecule (APP-MHC-I).

CONCLUSION: The efficacy of different IVIG on AD was significantly different, and only IVIG-C has been confirmed to possess significant neuroprotective effects, which are related to the inhibition of APP-MHC-I. IVIG may be a potential therapeutic for AD but further research is needed to evaluate the functional of IVIG before clinical trials of AD treatment.

Key words: Alzheimer's disease, intravenous immunoglobulin, neuroinflammation, antigen processing and presentation, MHC-I.

Introduction

Alzheimer's disease (AD), which is the most commonly occurring neurodegenerative disorder, is marked by gradual deterioration in cognitive function and changes in personality (1). The prevalence of AD is rising annually as the world's population ages (2). The number of AD sufferers is expected to hit 130 million by 2050, which will not only place a heavy psychological burden on patients' families but also leads to huge social and public expenditure (3). Current drugs for AD patients only ameliorate marginally cognitive deficits, so it's urgent to explore novel preventive interventions and therapeutics for AD.

Despite the fact that the etiology of AD is not yet fully understood, it is believed that the most important pathophysiological characteristics are extracellular β-amyloid (Aβ) deposition to form senile plaques and the formation of neurofibrillary tangles caused by intracellular hyperphosphorylated tau (p-tau) protein (4). Recent years have seen a growing body of research suggesting that AD development is significantly influenced by inflammation (5).

Intravenous immunoglobulin (IVIG) is derived from the plasma of multiple healthy donors, and more than 95 % of its components are human immunoglobulin. With its full spectrum of human antibodies and the function of inhibiting inflammation (6, 7), IVIG has been used to treat patients with autoimmune diseases for nearly 40 years and is safe and well-tolerated (8-11). In 2002, IVIG was shown by Dodel. et al. to contain anti-Aβ antibodies for the first time (12). Since then, a variety of AD-relevant antibodies were found in IVIG, including anti-tau antibodies and anti-advanced glycation end-product receptor antibodies (13, 14). Based on the existence of anti-AD-related antibodies and anti-inflammation function in IVIG, at least five randomized controlled trials of IVIG for patients with AD have been performed around the world since 2013 (15-19). Importantly, IVIG had shown inconsistent efficacy as a potential treatment for AD in these clinical trials. The underlying mechanism is unrevealed, but the impact of IVIG itself on the results of clinical trials for AD has not gotten enough attention. IVIG was prepared from the mixed plasma of healthy adults, so the ethnicity and geography of donors and the preparation processes of the manufacturers will have a great impact on the composition of IVIG, and then affect the biological function (20, 21). It has been found that there are significant differences in levels of subtypes of IgG, IgA and IgM in various IVIG, although 95% of the components are human IgG (22, 23). Additionally, the content of sialic acid that may possess anti-inflammatory properties is unlike in different IVIG products (24).

Received March 19, 2023
Accepted for publication April 19, 2023

Figure 1. Experimental design grouping

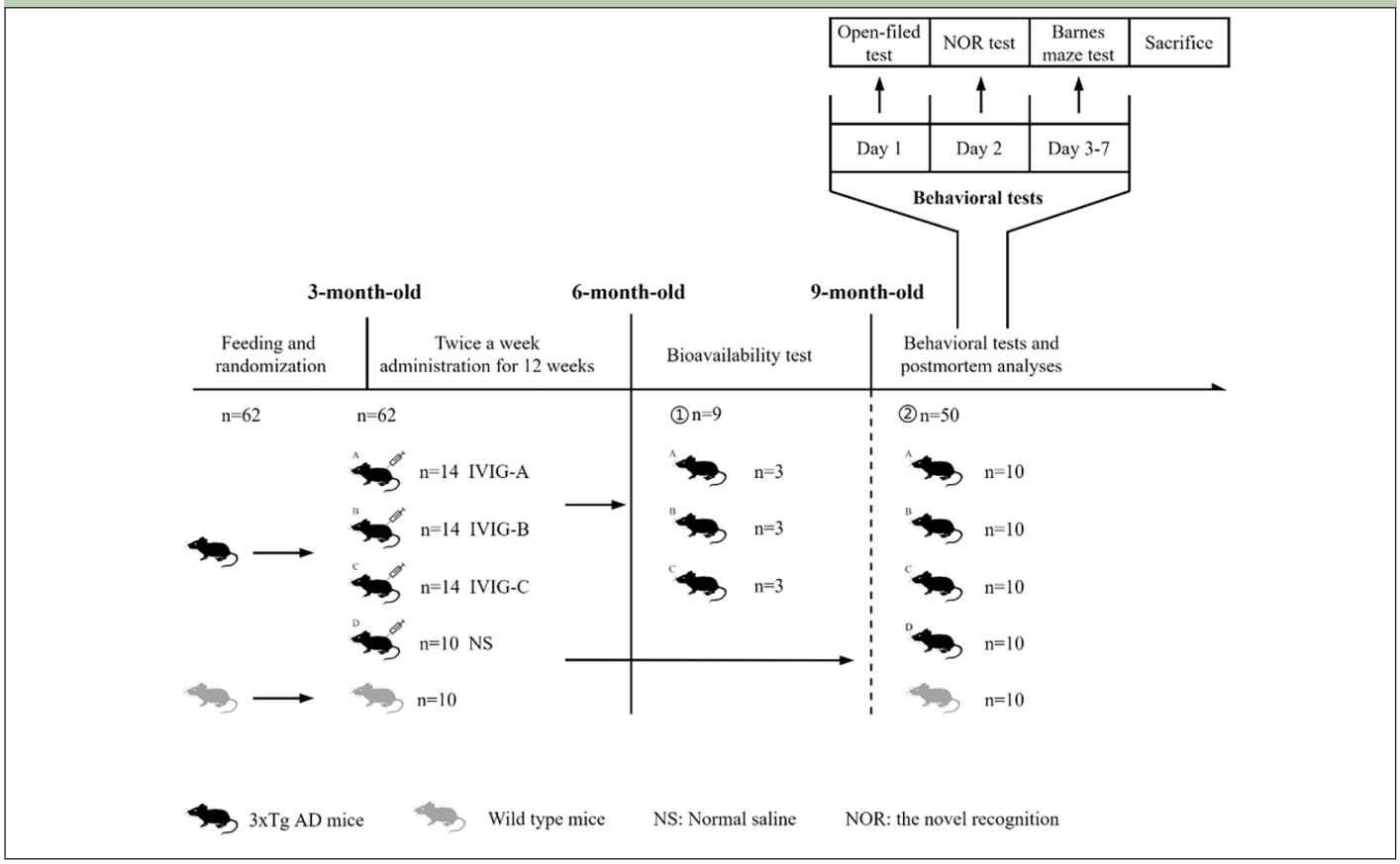

Therefore, the discrepancy in the therapeutic effects of different IVIG products on AD should be paid enough attention and need further study.

In the present study, we investigated the neuroprotective effects of IVIG from three different manufacturers in triple-transgenic (3xTg-AD) mice. Behavioral tests, Enzyme-linked immunosorbent assay (ELISA), Luminex, immunohistochemistry (IHC), proteomics and parallel reaction monitoring (PRM) were used to determine whether three IVIG had different efficacy on AD. Furthermore, the part of potential mechanisms of action was revealed. The results provide theoretical support for further investigation of the neuroprotective properties of IVIG, supply a preliminary analysis for inconsistent performance in different clinical trials of IVIG for AD treatment, and also offer a reference for the development of AD-specific IVIG.

Methods

IVIG selection

Three kinds of IVIG (5%, 50ml, 2.5g/bottle) numbered IVIG-A, IVIG-B and IVIG-C were selected for this study. These IVIG are produced by manufacturers located in north, northwest and south China respectively, and their preparation processes are not identical. In addition, the plasma donors of these manufacturers are great differences in race/ethnicity, geography and diet.

Animals and administration

The animal experiments were approved by the experimental animal ethics Chinese academy of medical sciences institute of blood transfusion (No. 2021048). A total of 52 3xTg-AD mice aged 10 weeks and weighing 13-17g were used in this study. They were obtained from Nanjing Biomedical Research Institute of Nanjing University, Jiangsu, China. Three mutant genes encoding human beta-amyloid precursor protein (APPswe), presenilin-1 (PS1M146V) and tau (P301L) were harbored in 3xTg-AD mice, which were used as AD models because of their expression of Aβ and tau pathology and cognitive deficits (25). A total of 10 age, weight and sex-matched C57BL6/J mice as wild-type (WT) mice were purchased from Hunan SJA Laboratory Animal Co., Ltd, Hunan, China. Briefly, the mice were raised under standard conditions (humidity: 50 ±10%, temperature: 22 ±2 °C, light/dark cycle: 12h) and food is available for random use. After 2 weeks of adjustable feeding, the 3xTg-AD mice were randomly divided into 4 groups (14 in per IVIG group, 10 in control group, half male and half female). The 3xTg-AD mice in the IVIG group (1g/kg, IVIG-A/B/C group) were intraperitoneally injected with three kinds of IVIG respectively, and the control

group (Ctrl group) was injected with the equivalent volume of normal saline twice a week for 12 weeks. Three mice were randomly selected from each IVIG group (IVIG-A/B/C group) to detect the bioavailability of IVIG following the last injection. After 3 months of normal feeding, the remaining mice (hereinafter referred to as 9-month-old mice) were tested using behavioral tests and then sacrificed. For biochemical, histopathological and proteomic assay, the serum and brain tissues were collected. The experimental design grouping are shown in Fig. 1.

Behavioral tests

Cognitive function was assessed for 3xTg-AD mice by a series of cognitive tests (Smart 3.0, Panlab, Spain). With a recuperation period of at least 24 hours between each task, behavioral assessments were carried out in the two weeks before the sacrifice to lessen stress.

A soundproof dark box (bottom area: 40 cm × 40 cm × 40 cm) was used for the open-field experiment test in order to evaluate the mice's autonomous activities in the novel environment (26). The automated recording of photobeam breaks was used to keep track of movements and calculate distance traveled. The movements of each mouse were tracked for 5 minutes in the open field. To remove any potential odor cues, the box was completely cleaned after each test.

Based on rodents' intrinsic desire for probing unfamiliar items, the novel object recognition (NOR) test was used to explore the memory and learning of mice (27). The mouse spent 5 minutes in a standard cage (bottom area: 40 cm × 40 cm × 40 cm) holding two identical items during the familiarization phase before being swiftly transferred back to its dwelling cage. A test of the animal's recognition memory was performed an hour later by showing it one familiar and one unfamiliar object. Each object's detection and sniffing time was recorded. The amount of time spent engaging with the new object relative to the whole amount of testing time was used to determine the NOR index.

Barnes maze test has been widely used to evaluate the memory of mice (28). The 3xTg-AD mice were tested individually over 5 days. Each mouse was put in the center of the maze and exposed to loud noises and strong light. The escape hole was left open for the mouse to utilize to depart the maze. Three trials lasting 3 minutes each were performed on training days 1 ~ 4 (The test interval was 20 minutes.). Mice underwent 3-minute probe trials on day 5. The hidden chamber was removed on the probe day. Mice were evaluated for their ability to remember the fixed position of a target hole. The time the animal stayed in the target zone where the escape hole was previously located was recorded during a 3-minutes probe trial. All tests took place at 7:00 ~ 11:30 a.m. for more consistency among mice.

Sample collection

Mice were chosen at random after behavioral testing, given a 2% sodium pentobarbital anesthesia, and then transcardially perfused with 0.9% sodium chloride and ice-cold 4% paraformaldehyde (PFA, BL539A; Biosharp life sciences, Shanghai, China). The brain tissues were carefully taken out, fixed in 4% PFA at 4 °C for 48 h and then incubated in 20% sucrose at 4°C for 72 h. The brain was cut into 25-μm thick slices and stained on a frozen microtome (RM2016, Leica Instrument Co., Ltd, Shanghai, China). For biochemical assays, the remaining mice were anesthetized to collect blood from the inferior vena cava, and the whole brain, hippocampus and parietotemporal cortex were dissected. The samples were immediately stored in -80 °C for further assay.

Enzyme-linked immunosorbent assay and Luminex

Human IgG (hIgG) concentrations were evaluated in the brain of 6-month-old 3xTg-AD mice using ELISA to assess the bioavailability of systemically administrated IVIG. The whole snap-frozen brain tissue was homogenized in lysis buffer and lysates were analyzed by species-specific ELISA kit (E-80G; ICL Lab, Oregon, America).

To detect soluble Aβ40 and Aβ42 levels in 3xTg-AD mice brain, the parietotemporal cortex was homogenized in cold PBS containing protease inhibitor cocktail and centrifuged at 15,000 g for 1 h at 4 °C. The supernatant was removed and became the soluble extract, which was determined using the bicinchoninic acid (BCA) protein assay (CW0014S; CWBIO, Beijing, China) according to the manufacturer's instructions. A portion of the supernatant was tested for Aβ40 and Aβ42 using the commercial high-sensitivity ELISA kit (Novus Biologicals, Colorado, USA). The other parts were quantified for 8 cytokines and chemokines using a commercially available Luminex kit (10014905, BIO-RAD, California, USA): Interleukins (IL)-1β, IL-2, IL-5, IL-6, chemokines (KC), IL-12P70, Tumor necrosis factor (TNF)-α and Interferon (IFN)-γ.

Immunohistochemistry

The slices were rinsed in PBS and treated in 3% hydrogen peroxide for 25 minutes before being blocked for nonspecific antigen binding with 3% BSA for 30 minutes at room temperature. Subsequently, the slices were incubated with primary antibodies against Aβ (Dilution ratio 1:500; NBP2-62566; Novus Biologicals, Colorado, USA), p-tau (Dilution ratio 1:200; 12885S; Cell Signaling Technology, Massachusetts, USA), glial fibrillary acidic protein (GFAP; Dilution ratio 1:2000; GB11096; Servicebio, Wuhan, China), and ionized calcium-binding adapter molecule 1 (Iba1; Dilution ratio 1:1000; GB113502; Servicebio, Wuhan, China) at

4 °C overnight. The slices were treated with the relevant secondary antibodies (HRP labeled) from the corresponding species of primary antibody (Dilution ratio 1:200; GB23303; Servicebio, Wuhan, China) at room temperature for 50 minutes the next day after being washed in PBS. The staining was developed with DAB color developing solution. Finally, the tissues were subjected to microscopic examination, and the extent of collagen deposition was quantitatively assessed using the Image J image analysis software (NIH Image J system, Bethesda, USA).

DIA proteomics

The hippocampal tissues obtained from the experimental mice were collected for proteomics. The tissues were ground into cell powder using liquid nitrogen, and four liters of lysis buffer (8M urea, 1% protease inhibitor cocktail; V900119-500G, Sigma-Aldrich, Germany) were then added. The cell powder was then sonicated three times on ice using a high-intensity ultrasonic processor (XM-900T, Scientz, Ningbo, China). Centrifugation was used to separate the residual debris for 10 minutes at 12,000 g and 4 °C. According to the manufacturer's instructions, the supernatant was collected, and the protein content was assessed using a BCA kit (P0011, Beyotime, Shanghai, China). The sample was slowly added to the final concentration of 20% (m/v) TCA (T4885-2KG, Sigma-Aldrich, Germany) to precipitate protein. The precipitate was collected by centrifugation at 4500 g for 5 min at 4 °C. The protein sample was then redissolved in 200 mM TEAB (T7408-500mL, Sigma-Aldrich, Germany) and ultrasonically dispersed. Trypsin (V5117, Promega, Wisconsin, USA) was added at 1:50 trypsin-to-protein mass ratio for the first digestion overnight. And then the peptides were desalted by Strata X SPE column. The sample was fractionated into fractions by high pH reverse-phase HPLC using Agilent 1260 Extend C18 column (5 μm particles, 4.6 mm ID, 250 mm length). The solvent A (2% acetonitrile/ in water, 0.1% formic acid; A117-50, Fluka, Germany) was used to dissolve the tryptic peptides before they were immediately length onto a homemade reversed-phase analytical column (25 cm long, 100 μm i.d.). With a nanoElute UHPLC system, peptides were separated using a gradient from 6% to 24% solvent B (0.1% formic acid in acetonitrile) over 70 min, 24% to 35% in 12 min, increasing to 80% in 4 min, and holding at 80% for the last 4 min (183793457696, Bruker, Germany).

Build spectral library: DDA (data-dependent acquisition) and DIA (data-independent acquisition) data were retrieved using pulsar search engine embedded in spectronaut software (v15.0) default parameters. The database was mus_sapiens_9606_SP_20220107.fasta (20387 sequences), added the reverse library to calculate the false positive rate (FDR) caused by random matching; FDR for protein, peptide and PSM identification was set to 1%. Processed with spectronaut software (v15.0), the corresponding spectral library was imported, and the retention time of peptide segments was predicted through nonlinear correction.

Parallel reaction monitoring

PRM has been widely used for the quantitative analysis of proteins (29, 30). And, it is an ion monitoring technique based on high-resolution, high-precision mass spectrometry that identifies and quantifies target proteins or peptides by selectively detecting them, such as peptides undergoing post-translational changes (31).

In the present study, PRM was used to verify the differential proteins in the hippocampus of mice in each group after the proteins were screened by DIA proteomics. The experimental method of protein extraction and trypsin digestion is the same as that of DIA proteomics. The peptides were separated by an ultra-high performance liquid phase system and injected into the capillary ion source for ionization and then analyzed by timsTOF Pro2 (187508710557, Bruker, Germany) mass spectrometry. Both the peptide mother ions and their secondary fragments were identified and examined at an ion source voltage of 1.65 kV. 100-1700 m/z was chosen as the secondary mass spectrometry scan range. A secondary spectrum of the number of precursion charges in the range of 0-5 was acquired using the parallel reaction monitoring–parallel cumulative serial fragmentation (prm-PASEF) mode in the data acquisition mode.

Secondary mass spectrometry data was retrieved using Maxquant (v1.6.15.0). Search parameter settings: The database was Mus_musculus_10090_SP_20220107.fasta (17097 sequences), a common contamination library was added to the database to remove the impact of contaminating proteins on the identification findings, and an anti-library was added to quantify the false-positive rate (FDR) brought on by random matching; Trypsin/P was used as the digesting technique; 2 was used as the number of missed cuts; The peptide's minimum length was set at 7 amino acid residues; The primary master ions' quality error tolerance for the first search and main search was set to 20 ppm and 4.5 ppm, respectively, while the secondary fragment ions' mass error tolerance was set at 20 ppm. The maximum number of peptide modifications was set at 5. Alkylated Carbamidomethyl (C) cysteine underwent a fixed modification, a variable modification to methionine oxidation, and acetylation at the protein's N-terminus. FDR was set to 1% for both protein and PSM identification.

The data were processed using Skyline 21.1 with the following peptide parameters: Trypsin [KR/P] as the protease, 0 for the maximum number of missing sites, 7 to 25 for the peptide length, and cysteine alkylation to fix modification. Mother ion charge is set to 2, daughter ion charge to 1, and ion type is set to b, y in the transition parameters. The mass error tolerance for ion matching

Figure 2. A) The hIgG concentrations in brain were evaluated in 3xTgAD mice after a 3-month intraperitoneal injection with IVIG (1 g/kg) using a specific ELISA. B) The hIgG concentrations in three kinds of IVIG were detected by the same ELISA kit. C) The percentage of hIgG of the brain in mice was calculated. Data are expressed as the mean ± SEM (n = 3)

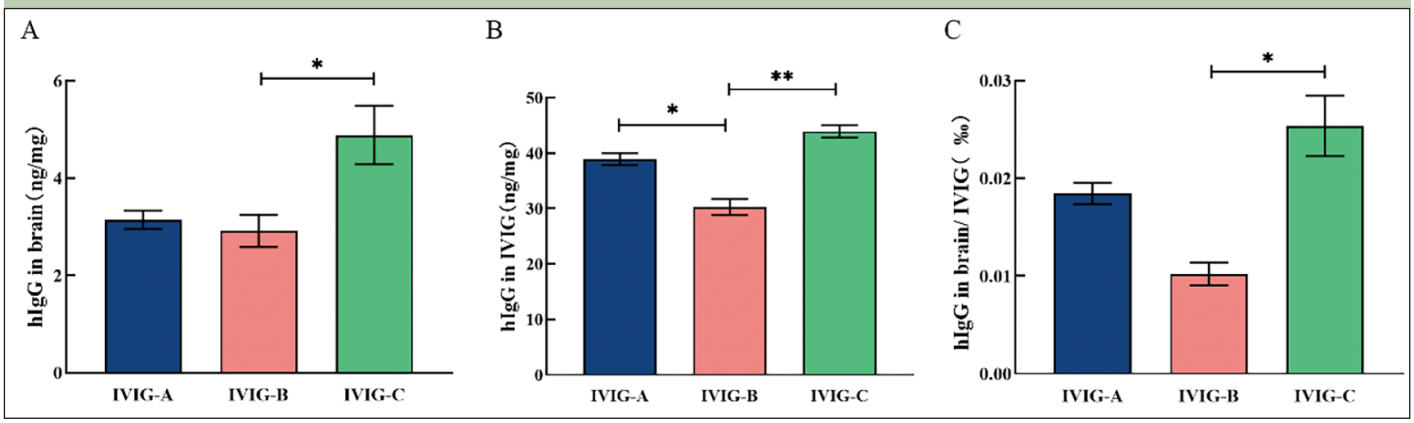

Statistical significance using one-way ANOVA is defined as * p<0.05, ** p<0.01. hIgG, Human IgG.

was set at 0.02 Da, and fragment ion selection went from the third to the last.

Statistical analysis

All data are presented as mean ± SEM and were analyzed with GraphPad Prism 9.0 (GraphPad Software Inc., San Diego, CA) using one-way ANOVA when appropriate, followed by post-hoc multiple comparisons (Dunn's test). * $p < 0.05$, * * $p < 0.01$, * * *$p < 0.001$.

Results

The Bioavailability of IVIG is different in 3xTg-AD mice

To measure the bioavailability of IVIG, 3 mice from each IVIG group (IVIG-A/B/C group) were randomly selected and sacrificed two hours after the last IVIG injection. The whole brain was taken to detect hIgG in three kinds of IVIG groups. There was no significant difference in hIgG concentrations of brain between IVIG-A and IVIG-B groups, but hIgG concentrations of brain in IVIG-C group were significantly higher than that in IVIG-B group ($p < 0.05$; Fig. 2A). The hIgG concentrations in three kinds of IVIG was detected by the same ELISA kit. The hIgG concentrations in IVIG-C ($p < 0.01$; Fig. 2B) and IVIG-A ($p < 0.05$; Fig. 2B) were significantly higher than that in IVIG-B. The percentage of hIgG of brain in mice was calculated and shown in Fig. 2C. The hIgG levels in brain/IVIG in IVIG-C group were significantly higher than that in IVIG-B group ($p < 0.05$; Fig. 2C). After intraperitoneal injection of IVIG into mice, the bioavailability of three IVIG was different. And IVIG-C entered the brain of mice with the largest amount of IgG.

IVIG improved cognitive decline in 3xTg-AD mice to different degrees

After the intraperitoneal injection of IVIG and saline and another 3 months of normal feeding, all mice were tested for cognitive behavior. the open-field experiment test was used to assess the mice's autonomous exploration behaviors and motor ability in a strange environment, as shown in Fig. 3A, D. The distance of movement in Ctrl group was significantly lower than that in WT group ($p < 0.05$), indicating that the 3xTg-AD mice traveled a less total distance in a new environment. However, the distance of movement in IVIG-A ($p < 0.0001$), IVIG-B ($p < 0.001$) and IVIG-C ($p < 0.05$) groups had a significant increase compared with Ctrl group. The mice's recognition memory was evaluated using NOR test (32), as shown in Fig. 3B, E. NOR index in Ctrl group was significantly lower than that in WT group ($p < 0.05$), indicating that the 3xTg-AD mice spent less time in exploring the novel object. However, NOR index in IVIG-C group had a significant increase compared with Ctrl group ($p < 0.05$). The mice's spatial memory and learning were evaluated using Barnes maze test (33), as shown in Fig. 3C, F. There was a significant difference in the time of staying in the target zone between Ctrl and WT groups ($p < 0.05$). Similarly, IVIG-C reversed the reduction of staying time in the target zone of 3xTg-AD ($p < 0.05$).

For 9-month-old 3xTg-AD mice, IVIG-C improved cognitive and motor decline in three behavioral outcomes (open-field experiment test, NOR test, Barnes maze test); IVIG-A and IVIG-B just improved the motor and autonomous decline in open-field experiment test.

IVIG failed to effectively modulate Aβ40 and Aβ42 concentrations in parietotemporal cortex of 3xTg-AD mice

In addition to the hippocampus, Aβ deposits were also found in the parietotemporal cortex of AD patients and mice, which aggravated cognitive impairment and

Figure 3. 3xTg-AD and WT mice were evaluated using open-field experiment test (A, D), NOR test (B, E), Barnes maze test (C, F) in 9-month-old (n = 8-10). IVIG counteracted the cognitive decline in 3xTg-AD mice to different degrees. Data are expressed as the mean ± SEM

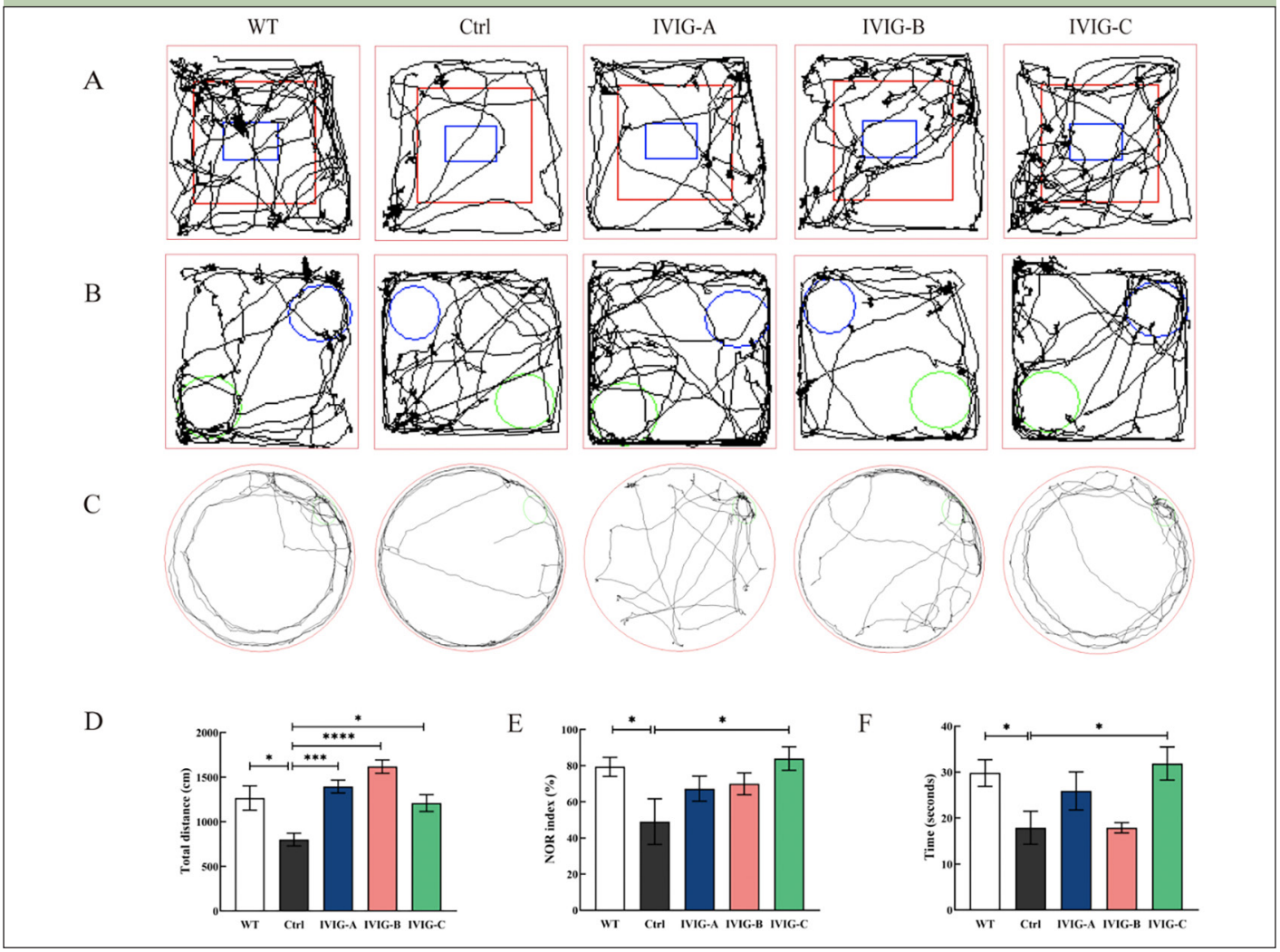

Statistical significance using one-way ANOVA is defined as * p<0.05, ** p<0.01, *** p<0.005, ****p<0.001. IVIG, intravenous immunoglobulin; WT, wild type; NOR, the novel object recognition.

Figure 4. The concentrations of soluble Aβ40 and Aβ42 were measured in parietotemporal cortex. It was found that just only IVIG-C decreased Aβ40 rather than Aβ42 concentrations in 9-month-old 3xTg-AD mice (A, B; n = 4). No significant changes in Aβ42/Aβ40 ratios were found in 3xTg-AD mice (C; n = 4)

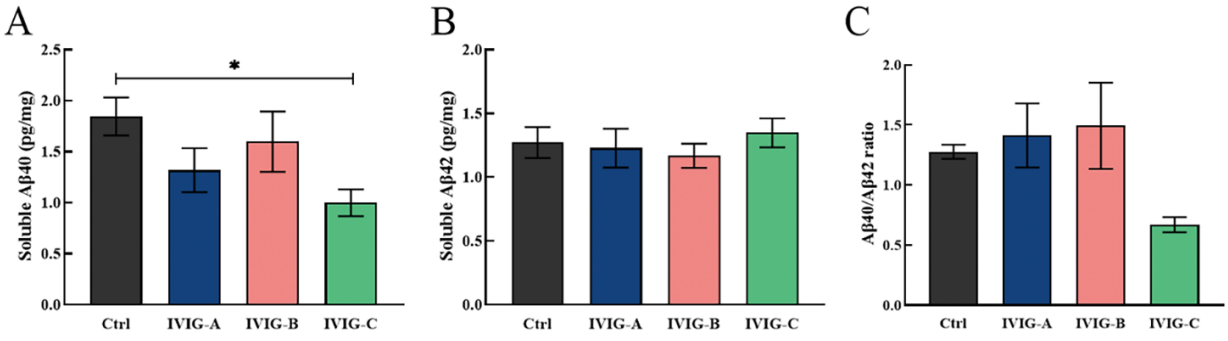

Data are expressed as the mean ± SEM. Statistical significance using one-way ANOVA is defined as * p<0.05, ** p<0.01, *** p<0.005, ****p<0.001. IVIG, intravenous immunoglobulin; WT, wild type; NOR, the novel object recognition.

Figure 5. Three IVIG ameliorated pathological alterations in the hippocampus to different degrees. IVIG-C reduced the deposition of Aβ in the hippocampus of 3xTg-AD mice, tested using 6E10 (A) in the hippocampus (50×; scale bar: 200μm; 100×; scale bar: 100μm; n= 3-4) and reduced the levels of p-tau (B). IVIG-A, IVIG-B and IVIG-C inhibited the levels of Iba1 (C) in the hippocampus of 3xTg-AD mice (50×; scale bar: 200μm; 100×; scale bar: 100μm; n = 3-4). IVIG-A and IVIG-C reduced the levels of GFAP (D) in the hippocampus of 3xTg-AD mice (50×; scale bar: 200μm; 100×; scale bar: 100μm; n = 3-4). Image J and Graphpad Prism were used for quantitative analysis of Aβ IHC staining area (E) and p-tau (F), microglia (G) and astrocyte number (H) in the hippocampus under 50× microscope. Data are expressed as the mean ± SEM

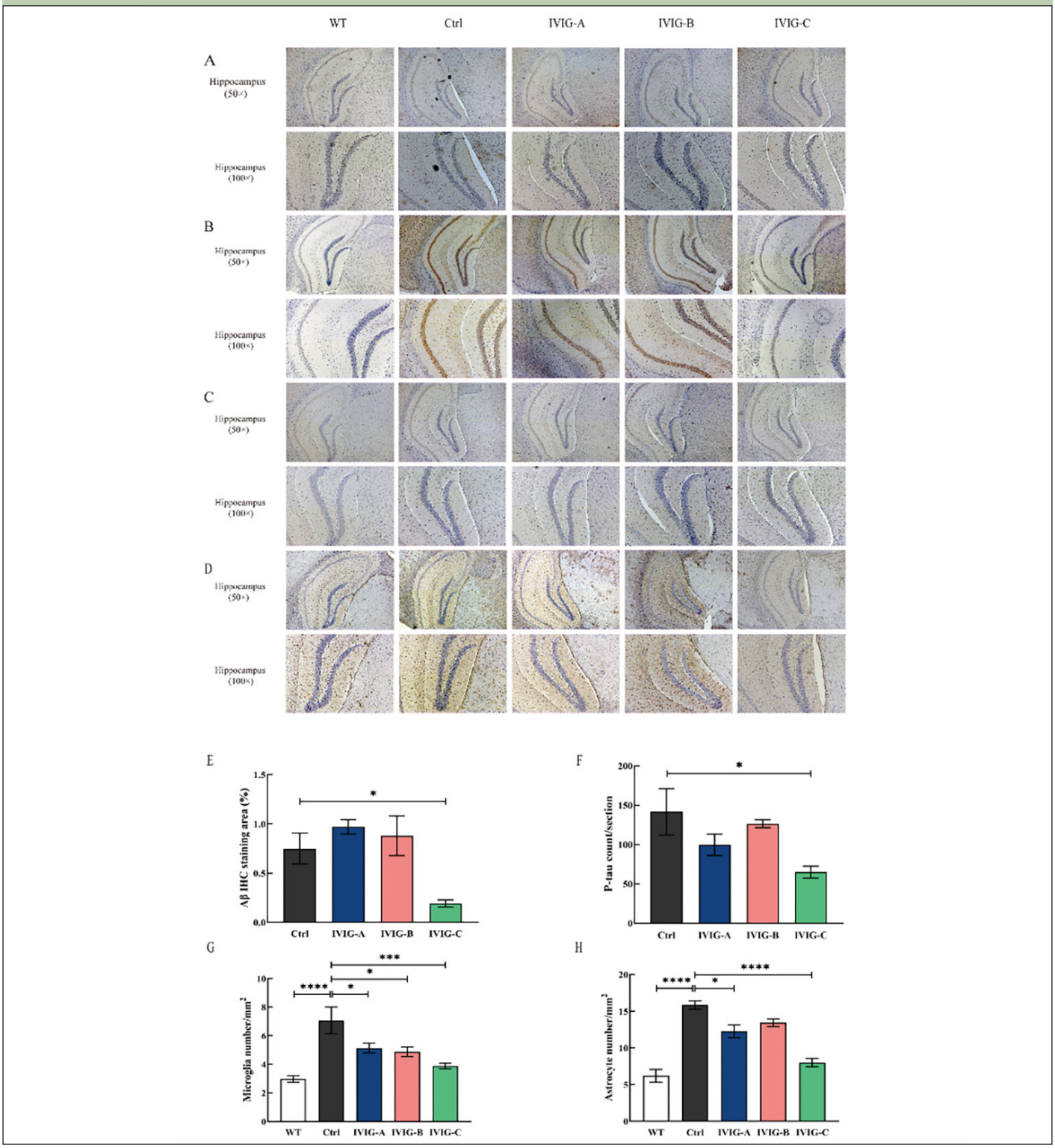

Statistical significance using one-way ANOVA is defined as * p<0.05, ** p<0.01, *** p<0.005, ****p<0.001. IVIG, Intravenous immunoglobulin; WT, wild type; IHC, immunohistochemistry; p-tau, phospho-tau protein; GFAP, glial fibrillary acidic protein; Iba1, ionized calcium-binding adapter molecule 1.

Figure 6. The effects of different IVIG on cytokines levels in the brains of mice. Data are expressed as the mean ± SEM (n = 8)

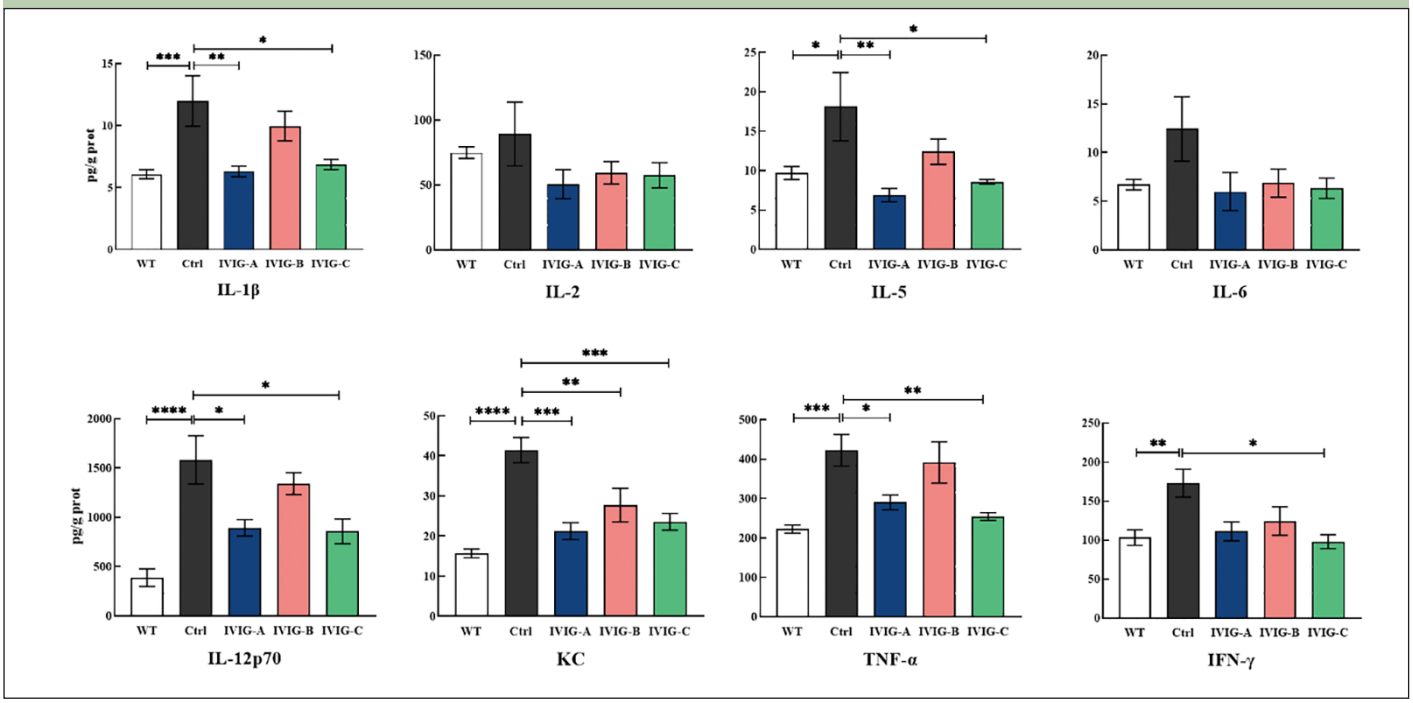

Statistical significance using one-way ANOVA defined as *p < 0.05, **p < 0.01, ***p < 0.001; IVIG, Intravenous immunoglobulin; WT, wild type; prot, proteins; KC, chemokines; IL, Interleukins; TNF, Tumor necrosis factor; IFN, Interferon.

disease progression (34, 35). The concentrations of soluble Aβ40 and Aβ42 were measured in parietotemporal cortex using specific ELISA. For 9-month-old 3xTg-AD mice, the concentration of Aβ40 in parietotemporal cortex was decreased by IVIG-C ($p<0.05$, Fig. 4A), while the concentrations of Aβ42 and Aβ42/Aβ40 ratios did not change significantly (Fig. 4B, C). These data indicated that IVIG failed to effectively modulate Aβ40 and Aβ42 concentrations in parietotemporal cortex of 3xTg-AD mice.

IVIG ameliorated pathological alterations in 3xTg-AD mice to different degrees

The autopsy was performed after the behavioral test of the mice at 9 months of age, and one side of the brain was taken for IHC staining. Aβ and p-tau is the most important pathogenic protein in the occurrence and development of AD (36). Several lines of evidence suggested that Aβ deposition may be required for the progression of tau pathology, neuroinflammation and cognitive impairment in AD (37). Tau stabilizes the cytoskeleton of neurons as a microtubule-associated protein, and hyperphosphorylation of tau may be a primary driver of neurodegeneration in AD (38). IHC showed that the area of hippocampal Aβ-positive plaques in the Ctrl group was significantly larger than that in the WT group, and the deposition of Aβ was alleviated in the hippocampus of 3xTg-AD mice by IVIG-C ($p < 0.05$, Fig. 5A, E) rather than IVIG-A and IVIG-B. The number of p-tau in the hippocampus of Ctrl group was significantly more than that of WT group, and the number of p-tau was reduced by IVIG-C ($p < 0.05$, Fig. 5B, F) rather than IVIG-A and IVIG-B. Neuroinflammation has been proven to be an important promoting factor in the progression of AD, and it's mainly reflected in the activation of microglia and astrocytes (39). Activated microglia and astrocytes are specifically identified by the biomarkers Iba1 and GFAP, respectively (40). In the hippocampus of the Ctrl group, there were more Iba1-positive GFAP-positive cells than in the WT group, and this increase was significantly reduced following IVIG-A($p < 0.05$), IVIG-B ($p < 0.05$) and IVIG-C ($p < 0.005$) treatment (Fig. 5C, G). The levels of GFAP (Fig. 5D, H) were decreased by IVIG-A ($p < 0.05$) and IVIG-C ($p < 0.001$).

All these data suggested that three kinds of IVIG ameliorated pathological alterations to different degrees in 9-month-old 3xTg-AD mice. And just IVIG-C not only reduced Aβ and tau in the hippocampus of 3xTg-AD mice but also suppressed the neuroinflammation in the brain.

IVIG regulated cytokine and chemokines levels in brain of 3xTg-AD mice to different degrees

Activated microglia and astrocytes release a large number of pro-inflammatory cytokines, leaving the brain in a state of inflammation, which can cause increased production of Aβ, damage to neurons and cognitive impairment (41). So, in order to evaluate whether IVIG could decrease the levels of cytokine and chemokines in

Figure 7. DIA proteomics was performed to evaluate the differential proteins after IVIG injection in the hippocampus of 3xTg-AD mice. (A) Proteins were differentially expressed between WT and Ctrl groups; Proteins were differentially expressed following IVIG-A (B), IVIG-B (C) and IVIG-C (D) treatment. GO enrichment analysis of Ctrl vs WT (E), IVIG-A vs Ctrl (F), IVIG-B vs Ctrl (G) and IVIG-C vs Ctrl group (H). Subcellular structure of differential protein enrichment in WT (I), IVIG-A (J), IVIG-B (K) and IVIG-C group (L)

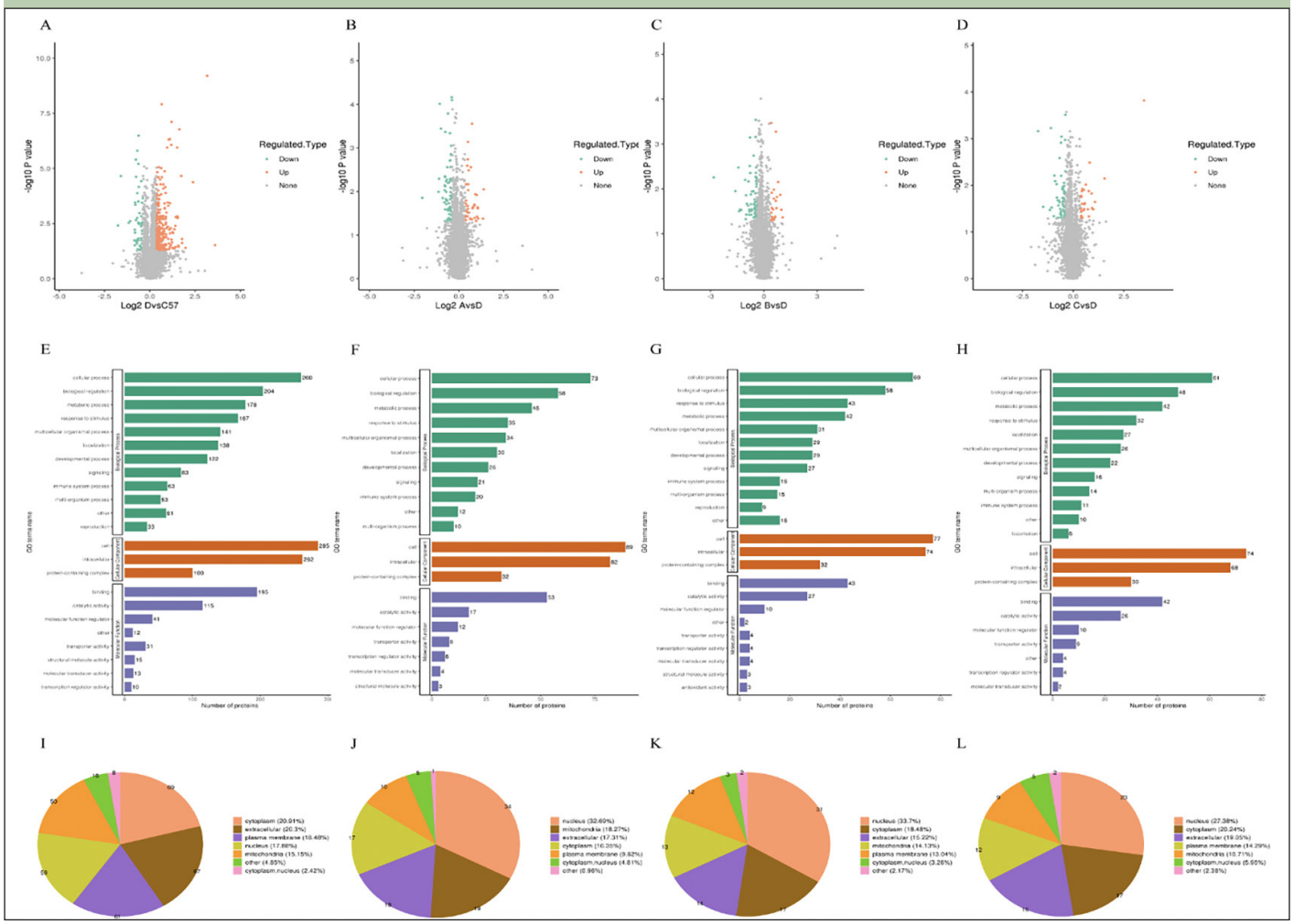

n = 3-4

the brain of 3xTg-AD mice, the levels of IL-1β, IL-2, IL-5, IL-6, KC, IL-12p70, TNF-α, IFN-γ were measured in the brain and shown in Fig. 6. The levels of IL-1β ($p < 0.001$), IL-5 ($p < 0.05$), KC ($p < 0.001$), IL-12p70 ($p < 0.001$), TNF-α ($p < 0.001$) and IFN-γ ($p < 0.01$) were markedly increased in the brain of Ctrl group compared with WT group. IVIG-A treatment significantly decreased the levels of IL-1β ($p < 0.01$), IL-5 ($p < 0.01$), KC ($p < 0.001$), IL-12p70 ($p < 0.05$) and TNF-α ($p < 0.05$) in the brain. IVIG-B treatment significantly decreased the levels of KC ($p < 0.01$) in the brain. And IVIG-C treatment significantly decreased the levels of IL-1β ($p < 0.05$), IL-5 ($p < 0.05$), KC ($p < 0.001$), IL-12p70 ($p < 0.05$), TNF-α ($p < 0.01$) and IFN-γ ($p < 0.05$) in the brain. Taken together, for 9-month-old 3xTg-AD mice, IVIG-A and IVIG-C could significantly better suppress the secretion of pro-inflammatory factors produced by activated glial cells than IVIG-B.

IVIG regulated protein levels in the hippocampus of 3xTg-AD mice to different degrees

The hippocampus was taken at 9 months of age from each group and subjected to proteomic analysis. After applying cut-off values of > 1.3 or < 0.77, we observed that 330 proteins were differentially expressed between WT and Ctrl mice (272 were upregulated and 58 were downregulated; Fig. 7A), and 104 proteins were differentially expressed following IVIG-A treatment (39 were upregulated and 65 were downregulated; Fig. 7B); 92 proteins were differentially expressed following IVIG-B treatment (24 were upregulated and 68 were downregulated; Fig. 7C); 84 proteins were differentially expressed following IVIG-C treatment (26 were upregulated and 58 were downregulated; Fig. 7D).

Figure 8. PRM was used to validate the differential proteins after IVIG injection in the hippocampus of 3xTg-AD mice. (A) The protein interaction image showed that proteins with significant differences in expression between IVIG-C and Ctrl groups may be closely related to APP-MHC-I. (B) A proteomics heatmap of WT, Ctrl, IVIG-A, IVIG-B and IVIG-C groups. Red represented high expression levels, and blue represented low expression levels. IVIG-C decreased the levels of the proteins related to APP-MHC-I via PRM: (C) The 10 differentially expressed proteins to be verified by PRM

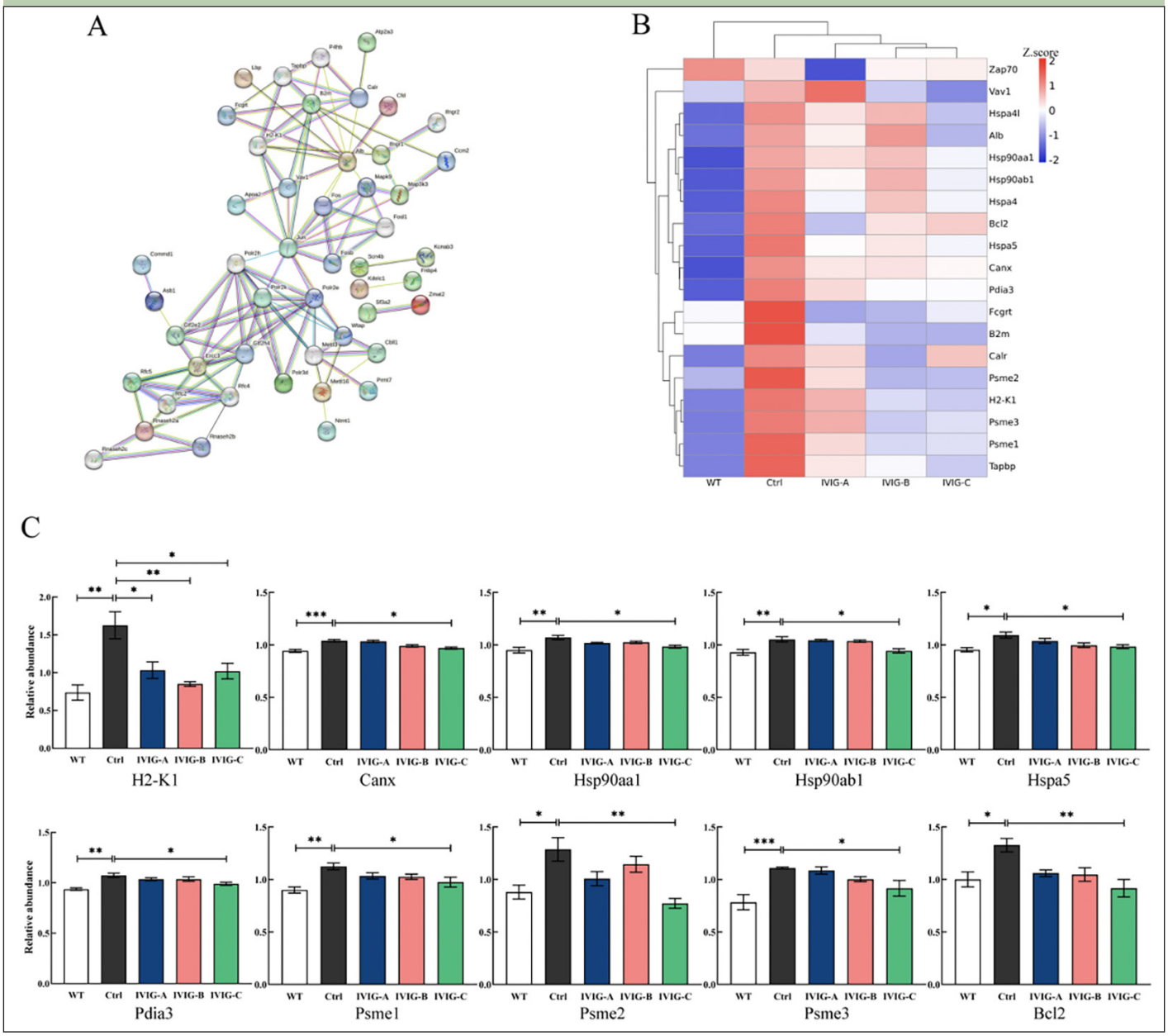

n = 3-4. Statistical significance using one-way ANOVA defined as *p < 0.05, **p < 0.01; IVIG, Intravenous immunoglobulin; WT, wild type.

Compared with Ctrl group, Gene Ontology analysis indicated an enrichment of mitochondrial organization proteins in Ctrl group (Fig. 7E), response to stimulus in IVIG-A group (Fig. 7F), response to bacterium in IVIG-B group (Fig. 7G), regulation of cytokine production in IVIG-C group (Fig. 7H). And PSORTb (v3.0) was used to annotate the subcellular structure of the proteins. Compared with Ctrl group, the differentially expressed proteins were mainly enriched in cytoplasm and extracellular in WT group (Fig. 7I), nucleus and mitochondria in IVIG-A group (Fig. 7J), nucleus and cytoplasm in IVIG-B group (Fig. 7K) and IVIG-C group (Fig. 7L).

IVIG-C downregulated the expressions of protein related to antigen processing and presentation by MHC class I molecules

STRING is a database of known and predicted protein-protein interactions, including both physical interactions as well as functional associations (42). We next used STRING to analyze interactions between 84 proteins that were differentially expressed between IVIG-C and Ctrl groups and found 104 enriched interactions and 77 expected interactions (Fig. 8A). Protein-protein interaction results showed that IVIG-C had a significant effect on antigen processing and presentation by MHC class I molecules (APP-MHC-I). In addition, IVIG-A had a significant effect on hematopoietic or lymphoid organ development (Supplementary. Fig. 1), and IVIG-B affected response to bacterium process (Supplementary. Fig. 2).

The differentially expressed proteins between Ctrl and IVIG groups were selected for cluster analysis. Compared with Ctrl mice, IVIG-C-treated mice had decreased concentration of proteins in the APP-MHC-I (Fig. 8B). APP-MHC-I is a wide range of immune processes and is essential for CD8 (+) T cell-dependent immune responses in organisms (43). Several studies have found that this immune pathway is associated with the progression of AD (44, 45). Ten proteins related to APP-MHC-I were confirmed in this study by proteomic screening and PRM. It is encouraging that IVIG-C was successful in regulating the APP-MHC-I signaling pathway as seen by the decrease in concentrations of H2-K1 ($p < 0.05$), Canx ($p < 0.05$), Hsp90aa1 ($p < 0.05$), Hsp90ab1 ($p < 0.05$), Hspa5 ($p < 0.05$), Pdia3 ($p < 0.05$), Psme1 ($p < 0.05$), Psme2 ($p < 0.01$), Psme3 ($p < 0.05$), Bcl2 ($p < 0.01$; Fig. 8C).

Discussion

It has been reported that IVIG can improve Alzheimer-like symptoms and protect neurons in mice by clearing Aβ disposition (46-48), upgrading complement anaphylatoxin C5a-mediated AMPA-CREB-C/EBP signaling pathway (49, 50), regulating fractalkine pathways (51), preservation of neuronal plasticity and tau phosphorylation homeostasis (52), respectively. However, its encouraging results in animal studies have not been replicated in larger clinical trials. In 2013, the randomized controlled trials with IVIG OctapharmaTM and IVIG GammagardTM gave disappointing results: In phase II clinical trial with IVIG OctapharmaTM (16), no significant differences were found in cognitive scores and the level of Aβ in the cerebrospinal fluid between the treatment group and the placebo group; In phase III trial with IVIG GammagardTM (53), no significant differences were detected between the IVIG and the placebo group for measures of cognitive functioning, despite the lowering of patients' brain levels of Aβ42. In 2017, Grifols conducted a phase II randomized controlled trial involving 52 patients with mild AD (15). After 12 months of IVIG treatment, the brain atrophy in the experimental group was found significantly less than that in the control group, and the cognitive function was significantly improved. Although the participants had a great influence on the results of clinical trials, the impact of IVIG products cannot be ignored. The inconsistency of results in these clinical trials prompted us to turn our attention to IVIG itself.

Our previous studies have found that there are significant differences in the antibody content and biological function of various IVIG from different manufacturers and even different batches, which was due to differences in the donors and preparation processes (20, 21, 54, 55). And the present study represents the first report on the effects of various IVIG on 3xTg-AD mice. We found that the efficacy of the IVIG on AD was significantly different. Three kinds of IVIG could alleviate cognitive decline, brain pathology and neuroinflammation to varying levels. This finding may provide possible explanations for the inconsistent results of clinical trials of IVIG for AD. In this study, only IVIG-C showed outstanding performance in improving Alzheimer-like symptoms, brain pathologies, and neuroinflammation in 3xTg-AD mice. This demonstrates that IVIG can regulate neuroinflammation in the brain and suppress the development of AD, and may be a potential therapeutic in the future.

The great number of injections raised the question of whether some effects might be related to mouse immune responses. But this was denied by several studies of IVIG treatment in AD mice, in which the autoimmune response of mice was often very mild (51, 56). Multiple shreds of evidence showed that IVIG can exert its role by penetrating the blood-brain barrier of 3xTg-AD mice (56, 57). In the present study, we also found that all three kinds of IVIG can pass through the blood-brain barrier, but IVIG-C entered the brain of 3xTg-AD mice with the largest amount of IgG. As the entry of IVIG into the central nervous system has not been quantified, it is still unknown whether this is a requirement for its effectiveness. We speculate that the different brain bioavailability of IVIG may be one of the reasons for the difference in its efficacy for AD.

Behavioral tests have been widely used to detect cognitive and behavioral abilities such as exercise, learning and memory in mice, including open-field experiment test for spontaneous exploratory movement, NOR test for learning and memory ability, and Barnes maze test for spatial memory and learning (58). 3xTg-AD mice have been shown to exhibit obvious cognitive and behavioral impairment at 5-6 months of age (59). We found that 3 kinds of IVIG produced significantly different behavioral improvements in 3xTg-AD mice. After 3 months of the administration and another 3 months of feeding, IVIG-C has the most significant effect on the cognitive function of 9-month-old 3xTg-AD mice as evidenced by the great improvement in open-field, NOR and Barnes maze day.

Accumulation of Aβ and phosphorylation of

tau are important central pathological features of AD (60). Dysregulation of the Aβ production, processing and clearance are considered to be the earliest and the most important events in the disease process (61). Aβ and its induced aggregation of p-tau lead to neuronal degeneration. The development of a chronic inflammatory response in the brain, known as neuroinflammation, is an early pathological alteration in AD (62). 3xTg-AD mice carrying human APP, PS1 and tau genes showed obvious Aβ deposition, p-tau accumulation and neuroinflammation at 6-7 months of age (59). At 9 months of age, we found that the effects of IVIG from different manufacturers on brain pathology were significantly different. IVIG-C showed significant improvement for 3xTg-AD mice in all pathological outcomes, including reducing the deposition of Aβ and p-tau in the hippocampus, reducing the number of activated microglia and astrocytes, and inhibiting the occurrence of cerebral neuroinflammation.

Neuroinflammation can increase taupathy and Aβ deposition in the brain, which in turn aggravates neuroinflammation (63, 64). IVIG has been proven to have a great anti-inflammatory effect (65). For 9-month-old 3xTg-AD mice, the effects of IVIG from different manufacturers on neuroinflammation were significantly different. IVIG-A and IVIG-C significantly better inhibit the secretion of pro-inflammatory factors released by activated glial cells than IVIG-B.

The therapeutic effect of IVIG-C group was the best in all experimental groups in this study. In this group, cognitive decline was improved, pathological alterations were ameliorated, proinflammatory cytokine and chemokines levels in brain were suppressed in 3xTg-AD mice. Therefore, we chose to perform hippocampal proteomics analysis on the IVIG-C group.

To search for proteins that were significantly differentially expressed, DIA quantification proteomics analysis was carried out. According to GO and KEGG pathway analyses, the immune response and antigen processing and presentation pathway was the GO category for the IVIG-C group that was most significantly impacted, which is consistent with the findings of cytokine and chemokine detection in the brain. In particular, proteins related to the function of the MHC class I protein were significantly downregulated in IVIG-C group. These data were verified by PRM, with APP-MHC-I expression significantly downregulated in the 3xTg-AD hippocampus. A connection between innate and adaptive immunity is made possible by the processing and presentation of antigen. By exposing the T-lymphocytes to the captured antigen in this crucial step, innate immune system components like macrophages or dendritic cells activate the adaptive immune response (66). Innate immunity and inflammation are well-known factors in the pathogenesis and progression of AD (67). Previous studies have demonstrated that the imbalance of APP-MHC-I signal pathway can induce neuroinflammation and accelerate AD symptoms in SD rats (45), and neuroprotective drugs can activate adaptive immunity by regulating APP-MHC-I signal pathway to play its beneficial role (68, 69). In our study, IVIG-C may reduce the immune response in the hippocampus by clearing Aβ or inhibiting neuroinflammation, thereby reducing the activation of innate immunity. Importantly, it was observed that innate immunity response aggravates in the hippocampus of 3xTg-AD mice, and IVIG-C attenuated the process and ameliorates Alzheimer-like symptoms, neuronal state and function. This implied that IVIG-C may modulate innate and adaptive immune homeostasis, thereby regulating immune responses and neuroinflammation in 3xTg-AD mice.

There are some limitations in this study. Firstly, IVIG is a plasma-derived product that contains multiple antibodies, which means IVIG may target molecules other than inflammation, so further study would be needed to measure and analyze the anti-inflammatory ability and AD-related antibody content of these IVIG. Secondly, it is not clear whether IVIG acts on brain cells directly by permeating the blood-brain barrier or indirectly reduces neuroinflammation by reducing peripheral inflammation. The use of APP-MHC-I reporter mice treated with IVIG could be a potential remedy for this problem. Thirdly, the results of this study cannot be determined that batches from the same manufacturer always respond similarly or are just randomly different. Therefore, the next step of the study is to evaluate different batches of IVIG from the same manufacturer. Finally, although our study supports that the downregulation of APP-MHC-I improved the progression of AD, further studies are needed to clarify the relationship between APP-MHC-I and AD. For example, it could be verified whether Aβ deposition is restored after APP-MHC-I activity of the hippocampus is resumed in 3xTg-AD.

In summary, this is the first study to report that IVIG from different manufacturers exhibited different neuroprotective effects in 3xTg-AD mice. And only IVIG-C showed overall improvement in neuroprotection, including alleviating cognitive decline, ameliorating Aβ deposition and tau phosphorylation, attenuating microglia and astrocyte activation, and inhibiting the secretion and expression of pro-inflammatory factors, thus restoring cognitive function. The neuroprotective effect of IVIG-C is related to the inhibition of APP-MHC-I signaling pathway.

The results suggest that IVIG showed promising therapeutic effects in AD treatment. Further study is needed to illustrate the molecular mechanism of IVIG-C against AD and the contribution of APP-MHC-I in the onset and progression of AD. Furthermore, functional evaluation for IVIG is extremely essential before clinical trials of AD treatment.

Acknowledgements: The authors have no acknowledgments to report.

Author's contributions: FZC and CHJ designed the experiments. FZC, BP, PRJ, YSL and DX performed the experiments. FZC, PRJ, WZK, ML, ZR and LCQ processed data. FZC and CHJ wrote the paper. FZC and CHJ revised the paper. All authors read and approved the final manuscript.

Funding: This work was supported by the Fundamental Research Funds for the Central Universities (Grant No. 3332022159). the Science and Technology Project of Sichuan (Grant No. 2019YFS0105); the Fundamental Research Funds for the Central Universities (Grant No. 3332018126); and the CAMS Innovation Fund for Medical Sciences (Grant No. CIFMS, 2021-I2M-1-060).

Availability of data and materials: The datasets used and/or analyzed during the current study are available from the corresponding author on reasonable request.

Ethics approval and consent to participate: Chinese academy of medical sciences institute of blood transfusion approved the experimental protocol (No. 2021048).

Consent for publication: Not applicable.

Competing interests: The authors declare that they have no competing interests.

References

1. Ossenkoppele R, Pijnenburg YA, Perry DC, et al. The behavioural/dysexecutive variant of Alzheimer's disease: clinical, neuroimaging and pathological features [J]. Brain, 2015; 138(9): 2732-49. https://doi.org/10.1093/brain/awv191.
2. Long JM, Holtzman DM. Alzheimer Disease: An Update on Pathobiology and Treatment Strategies [J]. Cell, 2019; 179(2): 312-39. https://doi.org/10.1016/j.cell.2019.09.001.
3. 2020 Alzheimer's disease facts and figures [J]. Alzheimers Dement, 2020; 16(3): 391-460. https://doi.org/10.1002/alz.12068.
4. Hindle A, Singh SP, Pradeepkiran JA, et al. Rlip76: An Unexplored Player in Neurodegeneration and Alzheimer's Disease? [J]. Int J Mol Sci, 2022; 23(11): 6098. https://doi.org/10.3390/ijms23116098.
5. Thu Thuy Nguyen V, Endres K. Targeting gut microbiota to alleviate neuroinflammation in Alzheimer's disease [J]. Advanced drug delivery reviews, 2022; 188: 114418. https://doi.org/10.1016/j.addr.2022.114418.
6. Fei Z, Chen Z, Du X, Cao H, Li C. Efficacy and Safety of Blood Derivative Therapy for Patients with COVID-19: A Systematic Review and Meta-Analysis [J]. Transfus Med Hemother, 2022; 382: 1-13. https://doi.org/10.1159/000524125.
7. Fei Z, Pan B, Pei R, et al. Efficacy And Safety of Blood Derivatives Therapy in Alzheimer's Disease: A Systematic Review And Meta-Analysis [J]. 2021; 11(1):256. https://doi.org/10.1186/s13643-022-02115-y.
8. Dalakas MC. Update on Intravenous Immunoglobulin in Neurology: Modulating Neuro-autoimmunity, Evolving Factors on Efficacy and Dosing and Challenges on Stopping Chronic IVIg Therapy [J]. Neurotherapeutics, 2021; 18(4): 2397-418. https://doi.org/10.1007/s13311-021-01108-4.
9. Bien CG. Management of autoimmune encephalitis [J]. Curr Opin Neurol, 2021; 34(2): 166-71. https://doi.org/10.1097/wco.0000000000000909.
10. Dilley M, Wangberg H, Noone J, Geng B. Primary immunodeficiency diseases treated with immunoglobulin and associated comorbidities [J]. Allergy Asthma Proc, 2021; 42(1): 78-86. https://doi.org/10.2500/aap.2021.42.200113.
11. Vani J, Elluru S, Negi V-S, et al. Role of natural antibodies in immune homeostasis: IVIg perspective [J]. Autoimmun Rev, 2008; 7(6): 440-4. https://doi.org/10.1016/j.autrev.2008.04.011.
12. Dodel R, Hampel H, Depboylu C, et al. Human antibodies against amyloid beta peptide: a potential treatment for Alzheimer's disease [J]. Ann Neurol, 2002; 52(2): 253-6. https://doi.org/10.1002/ana.10253.
13. Smith LM, Coffey MP, Klaver AC, Loeffler DA. Intravenous immunoglobulin products contain specific antibodies to recombinant human tau protein [J]. Int Immunopharmacol, 2013; 16(4): 424-8. https://doi.org/10.1016/j.intimp.2013.04.034.
14. Yan SS, Chen D, Yan S, et al. RAGE is a key cellular target for Abeta-induced perturbation in Alzheimer's disease [J]. Front Biosci (Schol Ed), 2012; 4(1): 240-50. https://doi.org/10.2741/265.
15. Kile S, Au W, Parise C, et al. IVIG treatment of mild cognitive impairment due to Alzheimer's disease: a randomised double-blinded exploratory study of the effect on brain atrophy, cognition and conversion to dementia [J]. J Neurol Neurosurg Psychiatry, 2017; 88(2): 106-12. https://doi.org/10.1136/jnnp-2015-311486.
16. Dodel R, Rominger A, Bartenstein P, et al. Intravenous immunoglobulin for treatment of mild-to-moderate Alzheimer's disease: a phase 2, randomised, double-blind, placebo-controlled, dose-finding trial [J]. Lancet Neurol, 2013; 12(3): 233-43. https://doi.org/10.1016/S1474-4422(13)70014-0.
17. Arai H, Ichimiya Y, Shibata N, et al. Safety and tolerability of immune globulin intravenous (human), 10% solution in Japanese subjects with mild to moderate Alzheimer's disease [J]. Psychogeriatrics, 2014; 14(3): 165-74. https://doi.org/10.1111/psyg.12055.
18. Relkin NR, Thomas RG, Rissman RA, et al. A phase 3 trial of IV immunoglobulin for Alzheimer disease [J]. Neurology, 2017; 88(18): 1768-75. https://doi.org/10.1212/WNL.0000000000003904.
19. Nct. Phase 3 IGIV, 10% in Alzheimer's Disease. 2012. Available online: https://clinicaltrials.gov/show/NCT01524887. Accessed 2 March 2023.
20. Ma L, Zhang W, Hou M, et al. Analysis of sialic acid levels in Chinese intravenous immunoglobulins by high-performance liquid chromatography with fluorescence detection [J]. Biomedical chromatography : BMC, 2019; 33(4): e4452. https://doi.org/10.1002/bmc.4452.
21. Ye S, Zeng R, Jiang P, et al. Concentrations of antibodies against β-amyloid 40/42 monomer and oligomers in Chinese intravenous immunoglobulins [J]. J Pharm Biomed Anal, 2017; 138:277-82. https://doi.org/10.1016/j.jpba.2017.02.024.
22. Colado A, Elías EE, Sarapura Martínez VJ, et al. Immunomodulatory effects of different intravenous immunoglobulin preparations in chronic lymphocytic leukemia [J]. Sci Rep, 2021; 11(1): 12926. https://doi.org/10.1038/s41598-021-92412-8.
23. Alagna L, Meessen J, Bellani G, et al. Higher levels of IgA and IgG at sepsis onset are associated with higher mortality: results from the Albumin Italian Outcome Sepsis (ALBIOS) trial [J]. Annals of intensive care, 2021; 11(1): 161. https://doi.org/10.1186/s13613-021-00952-z.
24. Kwon H, Crisostomo AC, Smalls HM, Finke JM. Anti-aβ oligomer IgG and surface sialic acid in intravenous immunoglobulin: measurement and correlation with clinical outcomes in Alzheimer's disease treatment [J]. PloS one, 2015; 10(3): e0120420. https://doi.org/10.1371/journal.pone.0120420.
25. Oddo S, Caccamo A, Shepherd JD, et al. Triple-transgenic model of Alzheimer's disease with plaques and tangles: intracellular Abeta and synaptic dysfunction [J]. Neuron, 2003; 39(3): 409-21. https://doi.org/10.1016/s0896-6273(03)00434-3.
26. Madison CA, Kuempel J, Albrecht GL, et al. 3,3'-Diindolylmethane and 1,4-dihydroxy-2-naphthoic acid prevent chronic mild stress induced depressive-like behaviors in female mice [J]. Journal of affective disorders, 2022; 309:201-10. https://doi.org/10.1016/j.jad.2022.04.106.
27. Wang D, Liu Y, Zhao D, et al. Plppr5 gene inactivation causes a more severe neurological phenotype and abnormal mitochondrial homeostasis in a mouse model of juvenile seizure [J]. Epilepsy research, 2022; 183:106944. https://doi.org/10.1016/j.eplepsyres.2022.106944.
28. Wen J, Li Z, Zuo Z. Postoperative Learning and Memory Dysfunction Is More Severe in Males But Is Not Persistent and Transmittable to Next Generation in Young Adult Rats [J]. J Neurosurg Anesthesiol, 2022; Online ahead of print. https://doi.org/10.1097/ana.0000000000000856.
29. Zheng K, Yin Y, Cao Y, et al. Proteomic and parallel reaction monitoring approaches to evaluate biomarkers of mutton tenderness [J]. Food Chem, 2022; 397:133746. https://doi.org/10.1016/j.foodchem.2022.133746.
30. Brzhozovskiy A, Kononikhin A, Bugrova AE, et al. The Parallel Reaction Monitoring-Parallel Accumulation-Serial Fragmentation (prm-PASEF) Approach for Multiplexed Absolute Quantitation of Proteins in Human Plasma [J]. Anal Chem, 2022; 94(4): 2016-22. https://doi.org/10.1021/acs.analchem.1c03782.
31. Lesur A, Dittmar G. The clinical potential of prm-PASEF mass spectrometry [J]. Expert Rev Proteomics, 2021; 18(2): 75-82. https://doi.org/10.1080/14789450.2021.1908895.
32. Chaney AM, Lopez-Picon FR, Serrière S, et al. Prodromal neuroinflammatory, cholinergic and metabolite dysfunction detected by PET and MRS in the TgF344-AD transgenic rat model of AD: a collaborative multi-modal study [J]. Theranostics, 2021; 11(14): 6644-67. https://doi.org/10.7150/thno.56059.
33. Yang L, Wu C, Li Y, et al. Long-term exercise pre-training attenuates Alzheimer's disease-related pathology in a transgenic rat model of Alzheimer's disease [J]. Geroscience, 2022; 44(3): 1457-77. https://doi.org/10.1007/s11357-022-00534-2.
34. Reseco L, Atienza M, Fernandez-Alvarez M, Carro E, Cantero JL. Salivary lactoferrin is associated with cortical amyloid-beta load, cortical integrity, and memory in aging [J]. Alzheimers Res Ther, 2021; 13(1): 150. https://doi.org/10.1186/s13195-021-00891-8.
35. López-Picón FR, Snellman A, Eskola O, et al. Neuroinflammation Appears Early on PET Imaging and Then Plateaus in a Mouse Model of Alzheimer Disease [J]. J Nucl Med, 2018; 59(3): 509-15. https://doi.org/10.2967/jnumed.117.197608.

36. Huang D, Cao Y, Yang X, et al. A Nanoformulation-Mediated Multifunctional Stem Cell Therapy with Improved Beta-Amyloid Clearance and Neural Regeneration for Alzheimer's Disease [J]. Adv Mater, 2021; 33(13): e2006357. https://doi.org/10.1002/adma.202006357.
37. Guo T, Zhang D, Zeng Y, et al. Molecular and cellular mechanisms underlying the pathogenesis of Alzheimer's disease [J]. Mol Neurodegener, 2020; 15(1): 40. https://doi.org/10.1186/s13024-020-00391-7.
38. Ossenkoppele R, Van Der Kant R, Hansson O. Tau biomarkers in Alzheimer's disease: towards implementation in clinical practice and trials [J]. Lancet Neurol, 2022; 21(8): 726-34. https://doi.org/10.1016/s1474-4422(22)00168-5.
39. Smirnov D, Galasko D. Dynamics of neuroinflammation in Alzheimer's disease [J]. Lancet Neurol, 2022; 21(4): 297-8. https://doi.org/10.1016/s1474-4422(22)00087-4.
40. Mahan TE, Wang C, Bao X, et al. Selective reduction of astrocyte apoE3 and apoE4 strongly reduces Aβ accumulation and plaque-related pathology in a mouse model of amyloidosis [J]. Mol Neurodegener, 2022; 17(1): 13. https://doi.org/10.1186/s13024-022-00516-0.
41. Leng F, Edison P. Neuroinflammation and microglial activation in Alzheimer disease: where do we go from here? [J]. Nat Rev Neurol, 2021; 17(3): 157-72. https://doi.org/10.1038/s41582-020-00435-y.
42. Szklarczyk D, Gable AL, Nastou KC, et al. The STRING database in 2021: customizable protein-protein networks, and functional characterization of user-uploaded gene/measurement sets [J]. Nucleic Acids Res, 2021; 49(D1): D605-D12. https://doi.org/10.1093/nar/gkaa1074.
43. Jongsma MLM, De Waard AA, Raaben M, et al. The SPPL3-Defined Glycosphingolipid Repertoire Orchestrates HLA Class I-Mediated Immune Responses [J]. Immunity, 2021; 54(1): 132-50.e9. https://doi.org/10.1016/j.immuni.2020.11.003.
44. Huang Y, Zhao Z, Wei X, et al. Long-term trihexyphenidyl exposure alters neuroimmune response and inflammation in aging rat: relevance to age and Alzheimer's disease [J]. J Neuroinflammation, 2016; 13(1): 175. https://doi.org/10.1186/s12974-016-0640-5.
45. Cao Z, Robinson RA. Proteome characterization of splenocytes from an Aβpp/ps-1 Alzheimer's disease model [J]. Proteomics, 2014; 14(2-3): 291-7. https://doi.org/10.1002/pmic.201300130.
46. Wang T, Xie XX, Ji M, et al. Naturally occurring autoantibodies against Aβ oligomers exhibited more beneficial effects in the treatment of mouse model of Alzheimer's disease than intravenous immunoglobulin [J]. Neuropharmacology, 2016; 105:561-76. https://doi.org/10.1016/j.neuropharm.2016.02.015.
47. Magga J, Puli L, Pihlaja R, et al. Human intravenous immunoglobulin provides protection against Aβ toxicity by multiple mechanisms in a mouse model of Alzheimer's disease [J]. J Neuroinflammation, 2010; 7:90. https://doi.org/10.1186/1742-2094-7-90.
48. Sudduth TL, Greenstein A, Wilcock DM. Intracranial injection of Gammagard, a human IVIg, modulates the inflammatory response of the brain and lowers Aβ in APP/PS1 mice along a different time course than anti-Aβ antibodies [J]. J Neurosci, 2013; 33(23): 9684-92. https://doi.org/10.1523/jneurosci.1220-13.2013.
49. Gong B, Pan Y, Zhao W, et al. IVIG immunotherapy protects against synaptic dysfunction in Alzheimer's disease through complement anaphylatoxin C5a-mediated AMPA-CREB-C/EBP signaling pathway [J]. Mol Immunol, 2013; 56(4): 619-29. https://doi.org/10.1016/j.molimm.2013.06.016.
50. Gong B, Levine S, Barnum SR, Pasinetti GM. Role of complement systems in IVIG mediated attenuation of cognitive deterioration in Alzheimer's disease [J]. Curr Alzheimer Res, 2014; 11(7): 637-44. https://doi.org/10.2174/1567205011666140812113707.
51. St-Amour I, Paré I, Tremblay C, et al. IVIg protects the 3xTg-AD mouse model of Alzheimer's disease from memory deficit and Aβ pathology [J]. J Neuroinflammation, 2014; 11:54. https://doi.org/10.1186/1742-2094-11-54.
52. Counts SE, Perez SE, He B, Mufson EJ. Intravenous immunoglobulin reduces tau pathology and preserves neuroplastic gene expression in the 3xTg mouse model of Alzheimer's disease [J]. Curr Alzheimer Res, 2014; 11(7): 655-63. https://doi.org/10.2174/1567205011666140812114037.
53. Alzforum. GammagardTM Misses Endpoints in Phase 3 Trial. Available online: http://www.alzforum.org/news/research-news/gammagardtm-misses-endpoints-phase-3-trial. Accessed 2 March 2023.
54. Du X, Wang Z, Lv Z, et al. Content of anti-β-amyloid(42) oligomers antibodies in multiple batches from different immunoglobulin preparations [J]. Biologicals, 2020; 65:25-32. https://doi.org/10.1016/j.biologicals.2020.02.004.
55. Ye S, Lei M, Jiang P, et al. Demonstration of the IgG antibody repertoire against the bacteria Escherichia coli in Chinese intravenous immunoglobulins [J]. J Pharm Biomed Anal, 2017; 133:8-14. https://doi.org/10.1016/j.jpba.2016.10.018.
56. Dubey S, Heinen S, Krantic S, et al. Clinically approved IVIg delivered to the hippocampus with focused ultrasound promotes neurogenesis in a model of Alzheimer's disease [J]. Proc Natl Acad Sci U S A, 2020; 117(51): 32691-700. https://doi.org/10.1073/pnas.1908658117.
57. St-Amour I, Paré I, Alata W, et al. Brain bioavailability of human intravenous immunoglobulin and its transport through the murine blood-brain barrier [J]. J Cereb Blood Flow Metab, 2013; 33(12): 1983-92. https://doi.org/10.1038/jcbfm.2013.160.
58. Nie L, Xia J, Li H, et al. Ginsenoside Rg1 Ameliorates Behavioral Abnormalities and Modulates the Hippocampal Proteomic Change in Triple Transgenic Mice of Alzheimer's Disease [J]. Oxidative medicine and cellular longevity, 2017; 2017:6473506. https://doi.org/10.1155/2017/6473506.
59. Hoffman JL, Faccidomo S, Kim M, et al. Alcohol drinking exacerbates neural and behavioral pathology in the 3xTg-AD mouse model of Alzheimer's disease [J]. International review of neurobiology, 2019; 148:169-230. https://doi.org/10.1016/bs.irn.2019.10.017.
60. Zhang H, Wei W, Zhao M, et al. Interaction between Aβ and Tau in the Pathogenesis of Alzheimer's Disease [J]. International journal of biological sciences, 2021; 17(9): 2181-92. https://doi.org/10.7150/ijbs.57078.
61. Mehdipour M, Skinner C, Wong N, et al. Rejuvenation of three germ layers tissues by exchanging old blood plasma with saline-albumin [J]. Aging (Albany NY), 2020; 12(10): 8790.
62. Schain M, Kreisl WC. Neuroinflammation in Neurodegenerative Disorders-a Review [J]. Current neurology and neuroscience reports, 2017; 17(3): 25. https://doi.org/10.1007/s11910-017-0733-2.
63. Cavanagh C, Wong TP. Preventing synaptic deficits in Alzheimer's disease by inhibiting tumor necrosis factor alpha signaling [J]. IBRO reports, 2018; 4:18-21. https://doi.org/10.1016/j.ibror.2018.01.003.
64. Hur J-Y, Frost GR, Wu X, et al. The innate immunity protein IFITM3 modulates γ-secretase in Alzheimer's disease [J]. Nature, 2020; 586(7831):735-740. https://doi.org/10.1038/s41586-020-2681-2.
65. Morales-Ruiz V, Juárez-Vaquera VH, Rosetti-Sciutto M, Sánchez-Muñoz F, Adalid-Peralta L. Efficacy of intravenous immunoglobulin in autoimmune neurological diseases. Literature systematic review and meta-analysis [J]. Autoimmun Rev, 2022; 21(3): 103019. https://doi.org/10.1016/j.autrev.2021.103019.
66. Lee MY, Jeon JW, Sievers C, Allen CT. Antigen processing and presentation in cancer immunotherapy [J]. J Immunother Cancer, 2020; 8(2): e001111. https://doi.org/10.1136/jitc-2020-001111.
67. Nam H, Lee Y, Kim B, et al. Presenilin 2 N141I mutation induces hyperactive immune response through the epigenetic repression of REV-ERBα [J]. Nat Commun, 2022; 13(1): 1972. https://doi.org/10.1038/s41467-022-29653-2
68. Evgen'ev M, Bobkova N, Krasnov G, et al. The Effect of Human HSP70 Administration on a Mouse Model of Alzheimer's Disease Strongly Depends on Transgenicity and Age [J]. J Alzheimers Dis, 2019; 67(4): 1391-404. https://doi.org/10.3233/jad-180987.
69. Gao Y, Hong Y, Huang L, et al. β2-microglobulin functions as an endogenous NMDAR antagonist to impair synaptic function [J]. Cell, 2023; 186(5):1026-1038.e20. https://doi.org/10.1016/j.cell.2023.01.021.

How to cite this article: Z. Fei, B. Pan, R. Pei, et al. Neuroprotective Effects of IVIG against Alzheimer' s Disease via Regulation of Antigen Processing and Presentation by MHC Class I Molecules in 3xTg-AD Mice. J Prev Alz Dis 2023;3(10):581-594; http://dx.doi.org/10.14283/jpad.2023.56